



ELSEVIER

Contents lists available at ScienceDirect

Nuclear Instruments and Methods in
Physics Research Ajournal homepage: www.elsevier.com/locate/nima

Application of two-photon absorption in PWO scintillator for fast timing of interaction with ionizing radiation

E. Auffray^a, O. Bugarov^b, M. Korjik^c, A. Fedorov^c, S. Nargelas^d, G. Tamulaitis^d,
S. Tikhomirov^b, A. Vaitkevicius^{d,*}^a CERN, Geneva, Switzerland^b Stepanov Institute of Physics, Minsk, Belarus^c Research Institute for Nuclear Problems, Belarus State University, 11 Bobruiskaya, 220030 Minsk, Belarus^d Semiconductor Physics Department and Institute of Applied Research, Vilnius University, Saulėtekio 9-III, LT-10222 Vilnius, Lithuania

ARTICLE INFO

Article history:

Received 2 April 2015

Received in revised form

20 August 2015

Accepted 8 September 2015

Available online 16 September 2015

Keywords:

Radiation detectors

Scintillators

Lead tungstate

Two-photon absorption

ABSTRACT

This work was aimed at searching for fast phenomena in scintillators in sub-10-ps range, a benchmark timing for the time response of radiation detectors in particle colliders. The pump-and-probe optical absorption technique with a tunable-wavelength parametric oscillator as the pump and a continuous-spectrum source as the probe beam was used to study lead tungstate PbWO₄ (PWO) single crystals. It is shown that the rise time of the probe pulse absorption induced by the pump pulse is shorter than the pump pulse width of 200 fs. The approximately linear dependence of the probe absorption on the pump pulse energy density evidences that the induced absorption is caused by two-photon absorption involving one probe and one pump photon. We demonstrate that the intensity of the induced absorption at certain wavelengths is influenced by gamma irradiation, provided that an appropriate light polarization is selected. The application of the irradiation-sensitive nonlinearity for fast timing in radiation detectors is discussed.

© 2015 CERN for the benefit of the Authors. Published by Elsevier B.V. This is an open access article under the CC BY license (<http://creativecommons.org/licenses/by/4.0/>).

1. Introduction

Currently, the development of the experiments at future high energy particle colliders is the main stream in experimental high energy physics. Since the interaction length, where the particle bunches collide, is small (e.g., ~30 cm in the Large Hadron Collider at CERN [1]), timing becomes the key issue in the detection of rare events. A good timing measurement requires detectors with a high time resolution. Unfortunately, the time resolution of the detectors currently used in high energy physics experiments is limited to 50–70 ps that is definitely insufficient for applications in high luminosity accelerators. The time resolution of the majority of modern detectors is limited by the time response of the signal generated after the relaxation of carriers produced during the interaction. For example, in scintillation materials, the emission occurs after the relaxation of hot carriers lasting approximately 1 ps and the consecutive transfer of the carriers to emission centers, which takes 100 ps and more [2]. The Cherenkov radiation in inorganic medium occurs as a result of its polarization by a fast charged particle within 10⁻¹² s; however, the small yield of this

radiation and the large dispersion of the optical path lengths for the light collected in the volume of the detectors do not allow for a better time resolution than that in scintillation detectors.

The target 10 ps timing is beyond the capabilities of the conventional scintillator detecting systems based on the excitation relaxation and transfer to emitting centers. This publication presents the results of an attempt to search for qualitatively novel approaches to ensure the time marks in the detection. The final design of the detecting system will depend on the optimal methods and materials for this purpose. As the first step, we propose the two-photon absorption as a phenomenon prospective for fast timing and demonstrate that the nonlinear response in PWO is influenced by gamma irradiation.

The scintillator interaction with ionizing radiation generates an instantaneous elastic impact via local displacement of the lattice atoms. First of all, the medium might be elastically polarized by the ionization inducing the generation of holes in the inner atom shells and hot electrons [3]. The electrons and holes form dipoles localized in close vicinity to the particle track. Thus, the lattice polarization occurs along the entire track.

Another process of lattice distortion is the impact displacement of atoms from their regular sites in the lattice which happens under the intense flux of electrons or X-rays as described in [4]. The impact displacement of matrix ions occurs in the case when

* Corresponding author.

E-mail address: augustas.vaitkevicius@ff.vu.lt (A. Vaitkevicius).

the energy (≤ 100 eV) passed to an ion is insufficient to knock it into an intersite position in the host matrix.

Finally, the generation of an ensemble of free carriers in the crystal is followed by transient phenomena related with the transformation of the ensemble of hot carriers into the system of thermalized carriers. It has been suggested using the transient phenomena (luminescence and absorption) in transparent dielectric materials to obtain a time tagging of the interaction of ionizing radiation with scintillator material [5]. The hot intraband luminescence resulting in emission of photons with energy below the band gap can be detected and used as the time mark. The major disadvantage of such time mark is a small yield of the hot intraband luminescence. In particular, experiments in CeF_3 excited by short UV laser pulses showed that the pulse energy of several microjoules is necessary to observe the absorption from the lowest excited state of Ce^{3+} ions [6]. This corresponds to an instantaneous energy release of 10–20 TeV per cm^3 . Actually, this energy deposit could be expected in the detectors in the experiments at future colliders like FCC [7].

We suppose that the most promising process among the fast phenomena discussed above is the elastic polarization due to the charge redistribution when the electrons are displaced and holes generated. The formation of a hole in the shell of an atom in the crystal lattice naturally results in the transformation of the atom environment due to charge compensation. Since these atom displacements are produced via interaction with phonons, the lattice distortion occurs on the time scale comparable with the period of lattice vibrations, i.e., within 10^{-14} – 10^{-12} s. This local distortion in the lattice results in the redistribution of the electron density in the conduction band in the close vicinity of the hole. The relaxation of the elastic polarization might proceed via different radiative and non-radiative channels. The key feature of the elastic polarization is its short time response, which makes it promising to use as an optically detectable time mark.

In this paper, we investigated the fast optical response in lead tungstate (PbWO_4 , PWO) scintillator by using a pump and probe technique with sub-picosecond time resolution. The influences of wavelength, pump intensity and light polarization were under study.

The effect of elastic polarization should, probably, be observed in many crystals; however, the strongest effect might be expected in compounds with the bottom of the conduction band formed by nd orbitals of the lattice cations. According to the crystal field theory, these orbitals are most sensitive to distortions of the crystal field in the vicinity of emitting centers. To enhance the effect, self-activated crystals with lattice cations acting as emission centers need to be selected. From this point of view, good candidates could be crystals like molybdates and tungstates, where the lattice-forming atom groups MeO_4^{2-} ($\text{Me}=\text{W}, \text{Mo}$) act also as luminescence centers [2]. The undistorted group MeO_4^{2-} has the point symmetry T_d ; therefore, any lattice distortions in the vicinity of MeO_4^{2-} will decrease its symmetry and, consequently, will impose an additional splitting of d states and a change in the electron density at the bottom of the conduction band. This should result in the transformation of the band-to-band absorption spectrum. The direct observation of the changes in the absorption spectrum is hindered by the strong band-to-band absorption. Thus, we used the pump and probe technique to detect it.

For our study, we selected lead tungstate crystal, because it is already well studied and extensively used in scintillation detectors [8,3]. The two-photon absorption of femtosecond laser pulses in PWO single crystal has recently been observed in our previous work [9]. The band gap of PWO at room temperature is 4.33 eV. Thus, a defect-free PWO crystal has no optical absorption in the visible region. However, two-photon absorption at the total energy

of the two absorbed photons close to 6 eV and above results in the excitation to the electronic states near the bottom of the conduction band. The bottom of the conduction band in PWO is formed by d orbitals of tungsten ions, and the density of states has two bands peaking at 5 and 6.5 eV [10]. According to the crystal field theory, the lowest peak corresponds to the triplet states 3T_1 and 3T_2 , while the upper one is formed with a strong contribution of singlet states 1T_1 and 1T_2 [11].

The density of electronic states in the conduction band was simulated in PWO crystal with various defects [10]. The generation of nonequilibrium electrons and holes by ionizing radiation might also be treated as instantaneous creation of electron- or hole-type defects with simultaneous formation of elastic polarization. Therefore, the wavelength dependence of the two-photon absorption due to the optical transitions from the ground state formed by the upper 1A_1 state in the valence band to the conduction band should be correlated with the change in the electron density of states in the conduction band, while the ionizing radiation should change the wavelength dependence of such absorption.

2. Experimental

The changes in the density of the electronic states in the conduction band were studied using the ultrafast optical pump and probe technique. Two-photon absorption involving one pump and one probe photon has been exploited. The pump and probe laser pulses were focused on the sample surface at a small angle (see more detailed description of the technique in Ref. [6]). The pump-induced changes in the probe absorption have been recorded. The change in the sample absorption in the units of the thousandths of optical density (mOD) was estimated as the decimal logarithm of the measured ratio between the intensities of the transmitted probe beam propagating with and without pump beam:

$$\text{Differential absorption [mOD]} = \log \left(\frac{I_{\text{with pump}}}{I_{\text{without pump}}} \right) \times 1000.$$

The time evolution of the changes is revealed by changing the delay between pump and probe beams. The nonlinear absorption takes place only in the sample volume where the pump and probe beams propagate through the crystal spatially overlap.

Two pump and probe setups were used in our study.

In the first setup, 140 fs long pulses of the second harmonic of $\text{Al}_2\text{O}_3:\text{Ti}^{3+}$ laser radiation were used as a pump with the wavelength fixed at 395 nm (3.15 eV). A white continuum in the range from 400 to 1100 nm was used for probe. The continuum was generated in a water cuvette by a split fraction of the fundamental laser radiation at 790 nm. The initial spectrum of the continuum had the shape of two exponentially decreasing wings on both sides of the laser line at 790 nm. The approximately white spectrum of the continuum was achieved using colored absorption filters. The setup is described in detail elsewhere [6,12].

The first setup was used to study the nonlinear absorption under ionizing radiation. Samples in a shape of $10 \times 10 \times 1$ mm³ plates were cut from high structural quality PWO single crystals meeting the CMS specifications [2,8] intentionally doped by lanthanum and yttrium at the total concentration of 100 ppm. The face edges of the plate were oriented along the crystallographic axes *b* and *c*, while the pump and probe beams propagated at small angles to the axis *a* (i.e., nearly perpendicularly to the plate surface). The light in the pump beam was polarized along the axis *b*. The polarization of the probe either coincided or was at 75° from the polarization of the pump beam. A shielded ⁵⁷Co source of ionizing radiation (122 keV, 2 mCi) was mounted at a distance of 1 cm from the plate surface. The plate size and the experiment

configuration enabled absorption of 90% of the gamma radiation energy in the geometry close to $1/4\pi$. The measurements have been carried out at room temperature with the irradiation source on and off.

The second setup was used for pump and probe experiments at different pump photon energies: 394 nm (3.15 eV), 360 nm (3.44 eV), 346 nm (3.58 eV), and 654 nm (1.9 eV). The nonlinear absorption was studied along the crystallographic axis a in 1 cm thick samples. The light in the probe beam was polarized either along the axis b or c . The system was based on a femtosecond Yb: KGW laser producing 200 fs pulses at 1030 nm with a repetition rate of 30 kHz. A small part of the fundamental radiation was passed through an opto-mechanical delay line, frequency doubled (515 nm) and focused by a 10 cm focal length lens onto a 5 mm thick sapphire plate to generate a broad spectrum (super-continuum) probe beam. The range between 350 and 530 nm was used for probing in our experiments. The major part of the fundamental laser beam was used to pump an optical parametric amplifier (OPA) continuously tunable in the range from 630 to 2600 nm. The OPA radiation was frequency doubled and used as a tunable-wavelength pump source. The intensity of the pump beam was attenuated by a neutral density filter wheel. The probe beam, tunably delayed in respect to the pump pulse, was dispersed by an imaging spectrograph and detected using a CCD camera. The spectral resolution of the system was 0.7 nm/pix. Since the continuum spectrum was not flat, the spectrum of the nonlinear absorption has been digitally normalized to obtain the response to a white spectrum probe.

3. Results and discussion

3.1. Fast nonlinear optical response due to two-photon absorption

The change in the optical density for the probe beam induced by the pump at the wavelength of 394 nm is presented in Fig. 1a. The shape of the response is basically similar to that reported in [9]. It has a short rise time, a decay with characteristic time constant of few picoseconds, and a faster decay afterwards. The fast decrease of the absorption at the rear part of the response could be explained by the separation in space of the pump and probe beams, which are impinging the sample surface at slightly different angles. The overlap volume in a thick sample depends on the wavelengths of the two beams due to the light velocity dispersion. Thus, the delay between the leading front and the rear part of the nonlinear absorption depends on the pump and probe wavelengths due to the light group velocity dispersion.

The leading edge of the differential transmittance is displayed in Fig. 1b for several wavelengths of the probe beam. The figure proves that the time response on the leading edge is limited by the laser pulse shape rather than by the material properties. Thus, the processes responsible for the nonlinear absorption happen on a femtosecond time scale.

Fig. 2 presents the differential optical absorption versus the energy density of the pump pulse at 394 nm for different wavelengths of the probe pulse delayed by 1 ps. The data for Fig. 2 were obtained in the experiment configuration with the electric field of the probing light parallel to the c axis ($E \parallel c$). Quite similar dependences have been observed in the $E \parallel b$ configuration (not shown in this paper). The observed dependences of the differential absorption of the probe signal with the pump pulse energy density are approximately linear. This is the experimental evidence that the absorption is caused by a two-photon absorption process involving one pump and one probe photon [13].

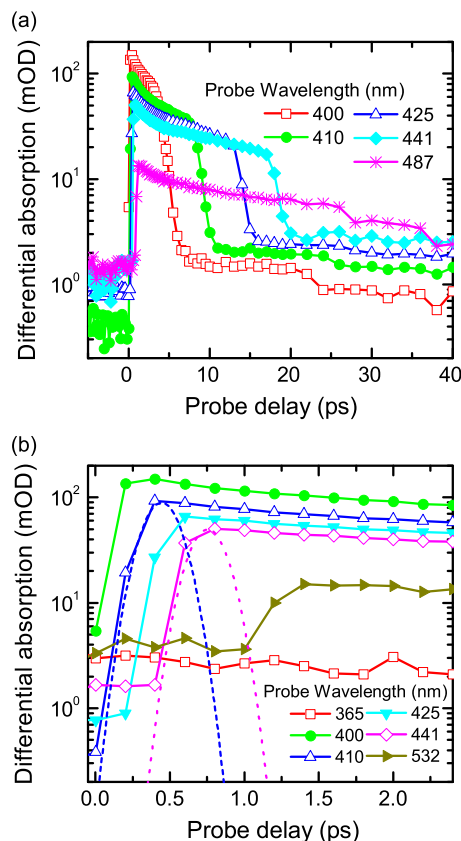


Fig. 1. Differential absorption (a) and the initial part of it (b) in PWO scintillation crystal at 394 nm pump and different probe wavelengths (indicated). The pump pulse shapes are depicted by dashed curves.

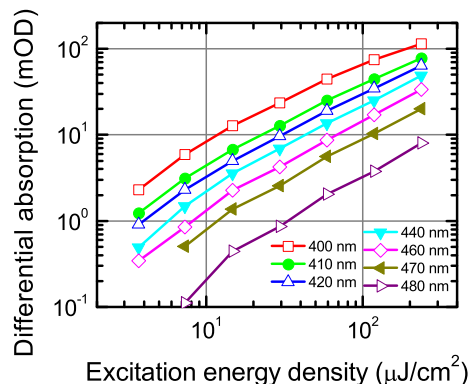


Fig. 2. Differential absorption versus energy density of pump pulse at 394 nm for different wavelengths (indicated) of the probe pulse delayed by 1 ps.

3.2. Influence of gamma irradiation on the nonlinear absorption

Fig. 3 presents the spectra of the differential absorption for different delays between pump and probe within the first 400 fs. Standard deviations of the data on the plots were estimated from spectra recorded at -1 ps probe pulse delay and found to be 1.9 mOD at 500 nm and 3 mOD at 700 nm wavelengths.

For the pump light polarization along the crystal axis b , the spectrum has a band peaking at ~ 3.13 eV (400 nm). Taking into account the pump photon energy of 3.15 eV (395 nm), the energy of the optical transition in this two-photon absorption is equal to 6.28 eV. This value is in agreement with our previous result observed in a crystallographically unoriented PWO crystal [6] and matches well with the energy of the second peak in the spectrum of the density of states calculated in [10]. When the pump light polarization is rotated

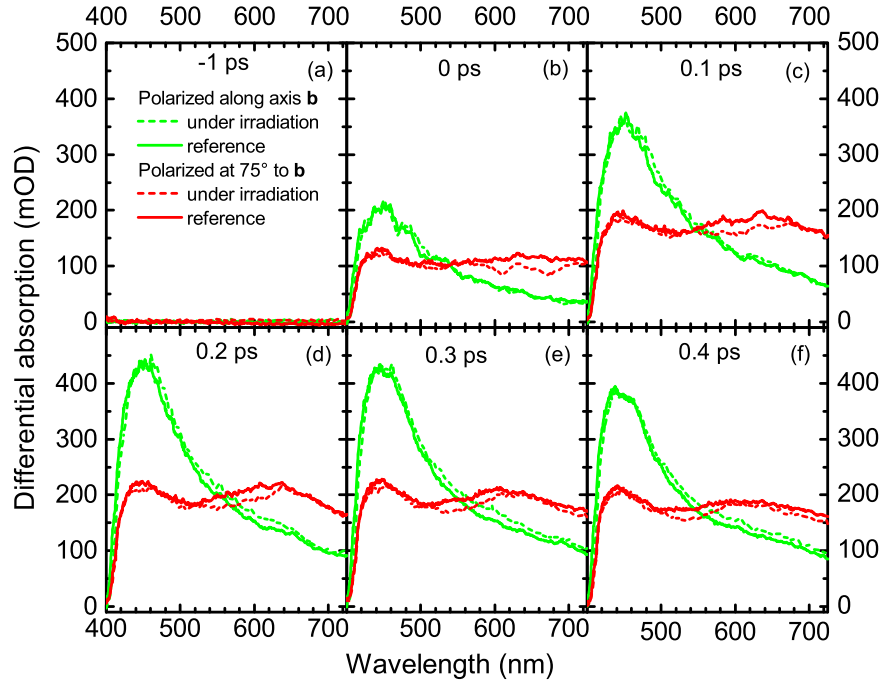


Fig. 3. Spectra of differential optical absorption induced by 500 mJ/cm² pump at 395 nm polarized along the crystal axis *b* and polarized at 75° to the crystal axis *b* (indicated) under (dashed lines) and without (solid lines) gamma irradiation. Delays of probe pulse are indicated.

away from the axis *b*, an additional band peaking at 2 eV (620 nm) appears simultaneously with the first band in the differential absorption spectrum. The peak position corresponds to the total transition energy of 5.15 eV and matches well with the low-energy band in the spectrum of the density of states [10].

The spectra in Fig. 3 were measured under and without gamma irradiation. No significant influence of the gamma irradiation was observed in the polarization configuration *E_b*, when only one band peaking around 450 nm in the differential absorption spectrum was observed. Meanwhile, certain damping of the low energy band peaking in the vicinity of 620 nm was observed under the influence of the irradiation in the second polarization configuration (see Fig. 3c and d). This change in the optical absorption could be used for the fast timing in radiation detectors.

We also observed a small change in the front shape of the response under irradiation; however, the change in the pulse shape is too weak to be exploited in a real detector.

Since the amplitudes of the electric field in the light wave of the probe and even pump (10³ V/cm) are considerably lower than the typical crystal field (10⁷–10⁸ V/cm), the pump and probe experiments do not induce significant distortion to the crystal symmetry including the structural polyhedrons. However, the situation considerably changes under ionizing radiation. The electrons generated from the inner atom shells move to a distance of up to several tens of microns during their thermalization. Meanwhile, the holes relax within distances comparable to the interatomic distance. As a result, an excessive positive charge is created along the track of the gamma or the particle in ionizing radiation. The electric dipoles form a low-symmetry component of the electric field, which acts in addition to the usual crystal field. As discussed above, this results in a redistribution of the electronic density. For example, the electric field of the dipole created by the hole and electron near the first coordination sphere of hole is proportional to the distance *r* as *r*⁻³ and reaches 10⁵–10⁷ V/cm at the distance of ~5 nm. A more accurate estimation of the electric field in the tracks requires application of the Ewald mathematical apparatus [14] and is outside the scope of the current publication.

Since the bottom of the conduction band in PWO is formed by polyhedrons WO₄²⁻, we can estimate the fraction of distorted polyhedrons in the crystal under irradiation used in our experiments. In our experimental conditions, not less than 3 × 10¹⁰ electron–hole pairs per second are generated by the gamma irradiation. The average track of the hot electron in PWO occupies a volume with approximately 0.2 μm in diameter and 40 μm in length, thus, ~0.4 × 10⁻¹² cm³ in volume. Accordingly, the total rate of the track volume formation is 1.2 × 10⁻² cm³ per second. Since the density of WO₄²⁻ polyhedrons in the PWO single crystal is ~10²² cm⁻³, the density of the polyhedrons within the volume of the irradiation-formed tracks equals approximately 10²⁰ cm⁻³. We should take into account that the lifetime of the elastic deformation is limited by the relaxation of free carriers. In PWO, the relaxation occurs via radiative recombination with a time constant of ~10 ns. Therefore, the non-equilibrium density of the polyhedrons distorted by irradiation is below 10¹² cm⁻³. This density seems to be too low for reliable detection. Thus, the crystal volume with polyhedrons distorted by elastic polarization supposedly extends outside the track volume. The dependence of the experimentally observed effect on the light polarization in respect to the crystallographic axes is an indication that the distortion of the low-symmetry structural polyhedrons is more effective along certain directions in the crystal matrix.

3.3. Nonlinear absorption as a function of pump photon energy

Depending on the combination of the wavelengths of the pump and the probe pulses, the absorption is caused by either two-photon or two-step absorption in the sample. In the latter case, the formation of a color center at the first absorption step might be expected. The major difference between these two absorption modes is that the two-photon absorption is an instantaneous process and takes place only if pump and probe pulses overlap in time inside the sample, while the time response in the two-step absorption depends on the population of real electronic states. The absorption from the state occupied after the absorption of the pump photon depends on the intra-state relaxation and the rate of

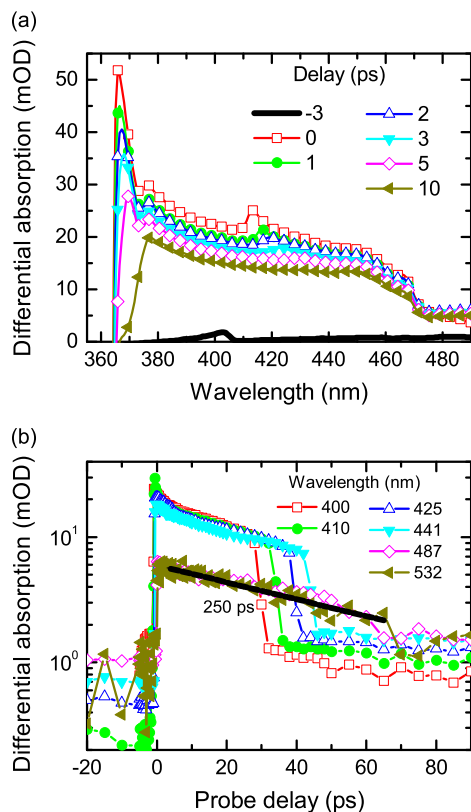


Fig. 4. Spectra (a) at different delays (indicated) and decay kinetics (b) at different wavelengths (indicated) of the differential absorption induced by pump at 360 nm (3.44 eV).

the color center recombination. It is well known [8] that point defects, particularly the oxygen vacancies (V_O), form a variety of shallow electron centers in $PbWO_4$ crystal with the thermal activation energy E_{TA} in the range from 0.029 to 0.7 eV. Two centers, WO_4^{3-} polaronic center ($E_{TA}=0.05$ eV) and $WO_4^{2-} + RE$ ($RE=Y, La$), were detected using electron paramagnetic resonance (EPR) at the temperatures of liquid nitrogen or lower. Thus, they should relax very fast at room temperature. Some other centers were detected only by means of the thermo-stimulated luminescence (TSL). They have no paramagnetic states, so it was supposed that they are stable after capturing two electrons and forming centers F ($V_O + 2e^-$). Consequently, the centers F^+ ($V_O + e^-$) in the host matrix do not become stable after capturing an electron [8].

As discussed above, the differential absorption induced by pump at 394 nm (3.15 eV) is caused by two-photon absorption. Meanwhile, the excitation involving electron transition to a real state close to the band gap was observed when the pump wavelength was shifted to 346 nm.

Fig. 4 presents the spectra at different delays and the decay kinetics at different wavelengths of the differential absorption induced by pump at 360 nm (3.44 eV). The experiments were performed in *EIIc* configuration for the light polarization. Fig. 4a depicts only the region of the high energy band, since the spectral range in the second setup used in these experiments was limited.

The decay kinetics of the induced absorption (Fig. 4b) is characterized by a fast increase, then a nearly exponential decay with the same rate for all probe wavelengths, a fast decrease due to separation of pump and probe in real space, and, finally, a slow decay with the time constant considerably exceeding the time scale in our experiments. The excitation of PWO at 360 nm delivers electrons to the deepest electron-type center in PWO, a Frenkel type defect (FTD), which is an oxygen vacancy V_O with a neighboring oxygen ion in the interstitial position. Capturing only

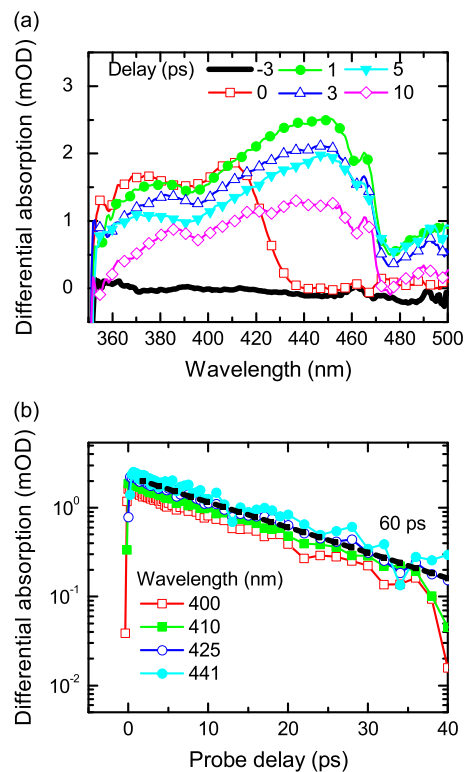


Fig. 5. Spectra (a) at different delays (indicated) and decay kinetics (b) at different wavelengths (indicated) of the differential absorption induced by pump at 346 nm (3.58 eV) in *EIIc* configuration.

one electron at this center does not form a stable color center [2]. Thus, the observed fast kinetics with 250 ps time constant for the induced probe absorption decay (see Fig. 4) is probably determined by subsidence of FTDs charged with one electron.

Moreover, the induced absorption is still observed even after the long delays (exceeding tens of picoseconds), when the pump and probe beams do not overlap in space and the probe absorption is influenced just by the carriers excited by probe photons. This behavior is in agreement with the transient absorption observed in PWO under excitation with nanosecond laser pulses [15].

As shown in Fig. 5a, the differential absorption is considerably weaker and its spectrum changes substantially when the pump wavelength is shifted to 346 nm (3.58 eV). In contrast to the spectra induced by the photons of smaller energy, no band corresponding to two-photon absorption is observed. Instead, two broad, strongly overlapping bands peaking at 380 and 410 nm appear at zero delay. At delays above 1 ps, a short wavelength wing of a new broad band (with the peak obviously beyond the spectral range of our experiment) is observed. The new band probably evidences that, in addition to FTD, V_O -based centers are populated with electrons generated by pump. Similarly as for FTDs, capturing of one electron does not ensure the stability of these centers. As a result, the induced absorption decreases with time delay. The kinetics presented in Fig. 5b show that the decay is exponential with a time constant of 60 ps. The decay is caused by the electron relaxation to the bottom of the state or by trapping of the electrons to deeper defect-related states.

It is worth noting that the light polarization in respect to the crystallographic axes is practically unimportant when color centers are involved in the process. Fig. 6 presents the spectra and kinetics of the differential absorption induced by pump in *EIIb* configuration. Comparison with the corresponding results obtained in *EIIc* configuration (see Fig. 5) shows that the spectra are quite similar and the decay kinetic is characterized by time constants of the same order of magnitude (60 and 25 ps) in both configurations.

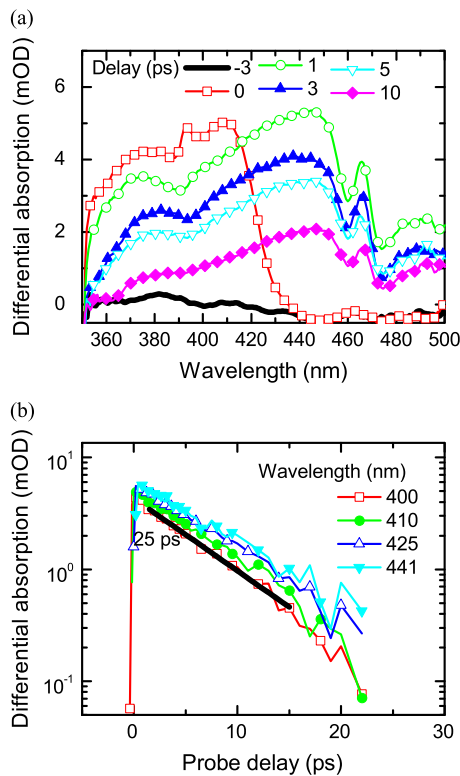


Fig. 6. Spectra (a) at different delays (indicated) and decay kinetics (b) at different wavelengths (indicated) of the differential absorption induced by pump at 346 nm (3.58 eV) in E_{11b} configuration.

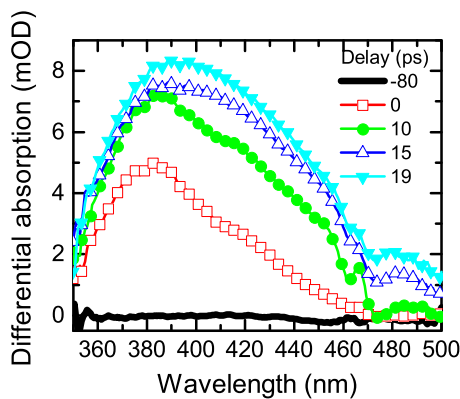


Fig. 7. Spectra at different delays (indicated) of the differential absorption induced by pump at 654 nm (1.9 eV).

The spectrum of the differential absorption at pump photon energy of 1.9 eV (654 nm) is presented in Fig. 7. The spectrum has two overlapping bands peaking at 380 and 410 nm and is similar to that obtained for UV pump at 3.58 eV (346 nm). Probably, the same centers are populated by absorption of a single 3.58 eV photon and by two-photon absorption of 1.9 eV photons.

The dependence of the spectral and time properties of the differential absorption on pump wavelength discussed above demonstrates that the selection of the proper wavelength to observe the nonlinear response from PWO crystals without population of defect-related states is of importance for implementation of this material in fast radiation detection systems.

3.4. Applications in detection of ionizing radiation

The effects observed in our study might be exploited for detection of ionizing radiation in parallel with the detection of

scintillation signal in the same material. The two-photon absorption can be used as a time tag to detect the initial moment of the interaction of ionizing radiation with the detector material, while the scintillation signal provides information on the absorbed energy. In the case of PWO, the wavelength of 500 nm corresponding to the total energy of two photons of 5 eV would be optimal.

The light propagating along the scintillation crystal and reflecting from the front face of the crystal could be used to observe the two-photon absorption. This configuration would also reduce the problems of the spatial overlap of the beams. Particularly, we consider this approach to be suitable for application in inorganic scintillation fibers in the detecting modules of SPOCAL or dual readout types [16,17]. The detection could be technically achieved by using a set of sub-picosecond pulses, e.g. 100 pulses with the total set duration of 0.1–1 ns. The set is injected into the crystal or fiber slightly before the time when the interaction products of the collision are expected to reach the detector modules. The laser pulses should be injected not in all fibers of the detecting modules but just to the specialized fibers in the module which are used for timing. The initial moment of the interaction between the collision products and the detector module is detected by comparing the set of pulses reflected back out of the crystal and a reference set. Thus, introducing the set of laser pulses with short spacing in the detecting module establishes a short-period time scale. The time resolution would be equal to the time span between the pulses in the set.

The radiation-induced changes either in spectral or time properties of the optical response could be exploited in the detectors. Further study is necessary to make the right choice ensuring a higher detection accuracy. The results obtained in our work are in favor of the exploitation of the change in the amplitude of the response at certain wavelengths.

The influence of ionizing radiation on the parameters of the two-photon absorption, which we observe in PWO crystal, should be observed also in other crystals and, probably, amorphous materials. The figures of merit for selection of the prospective materials should be a high point symmetry of the polyhedrons of metal ions forming the bottom of the conduction band, a high optical transparency at the wavelength used in the detection, and a high density of d-type electronic states in the lower part of the conduction band. The materials suitable for fabrication in a fiber shape have some additional advantages. Moreover, the experience accumulated on the propagation of ultrashort laser pulses in waveguides could be exploited in the development of such ultrafast detectors.

Acknowledgment

This work was carried out in the frame of the Crystal Clear Collaboration and the COST Action FAST (TD1401). Authors appreciate the fruitful discussions of the results and valuable remarks of Prof. A. N. Vasiliev. The study at Vilnius University was funded from the European Community's Social Foundation under Grant Agreement VP1-3.1-ŠMM-08-K-01-004/KS-120000-1756.

References

- [1] L. Evans, P. Bryant (Eds.), *The CERN Large Hadron Collider: Accelerator and Experiments*, Vol. 1–2, CERN, Geneva, 2009.
- [2] P. Lecoq, A. Annenkov, A. Gektin, M. Korzhik, C. Pedrini, *Inorganic Scintillators for Detector Systems*, Springer, Berlin, 2006.
- [3] G.M. Sessler (Ed.), *Electrets*, Springer-Verlag, Berlin, 1980.
- [4] V.I. Baryshnikov, T.A. Kolesnikova, *Physics Solid State* 47 (2005) 1776, <http://dx.doi.org/10.1134/1.2087734>.

- [5] P. Lecoq, M. Korzhik, A. Vasiliev, IEEE Transactions on Nuclear Science NS61 (2014) 229, <http://dx.doi.org/10.1109/TNS.2013.2282232>.
- [6] E. Auffray, O. Buganov, A. Fedorov, M. Korjik, V. Mechinsky, A. Tikhomirov, A. Vasil'ev, P. Lecoq, Journal of Instrumentation 9 (2014) P07017, <http://dx.doi.org/10.1088/1748-0221/9/07/P07017>.
- [7] W. Barletta, M. Battaglia, M. Klute, M. Mangano, S. Prestemon, L. Rossi, P. Skands, Nuclear Instruments and Methods in Physics Research A 764 (2014) 352, <http://dx.doi.org/10.1016/j.nima.2014.07.010>.
- [8] A.A. Annenkov, M. Korzhik, P. Lecoq, Nuclear Instruments and Methods in Physics Research A 490 (2002) 30, [http://dx.doi.org/10.1016/S0168-9002\(02\)00916-6](http://dx.doi.org/10.1016/S0168-9002(02)00916-6).
- [9] E. Auffray, O. Buganov, A. Fedorov, M. Korjik, P. Lecoq, G. Tamulaitis, S. Tikhomirov, A. Vasil'ev, Journal of Physics: Conference Series 587 (2015) 012056, <http://dx.doi.org/10.1088/1742-6596/587/1/012056>.
- [10] Y. Zhang, N.A.W. Holzwarth, R.T. Williams, Physical Review B 57 (1998) 12738, <http://dx.doi.org/10.1103/PhysRevB.57.12738>.
- [11] R. Kebabcioglu, A. Müller, Chemical Physics Letters 8 (1970) 59 0.1016/0009-2614(71)80575-4.
- [12] V.I. Stsiapura, A.A. Maskevich, S.A. Tikhomirov, O.V. Buganov, The Journal of Physical Chemistry A 114 (2010) 8345, <http://dx.doi.org/10.1021/jp105186z>.
- [13] J.-C. Diels, W. Rudolph, Ultrashort Laser Pulse Phenomena, Elsevier, USA, 2006.
- [14] (a) S.W. de Leeuw, J.W. Perram, E.R. Smith, Proceedings of the Royal Society of London A 373 (1980) 27;
(b) S.W. de Leeuw, J.W. Perram, E.R. Smith, Proceedings of the Royal Society of London A 373 (1980) 57.
- [15] D. Millers, S. Chernov, L. Grigorieva et al., Luminescence and transient absorption of doped PWO scintillator crystals, in: V.V. Mikhailin (Ed.), Proceedings of the Fifth International Conference on Inorganic Scintillators and their Applications, SCINT99, Moscow University, Moscow, 2000, pp. 613–618.
- [16] N. Luccini, T. Medvedeva, K. Pauwels, C. Tully, A. Heering, C. Dujardin, K. Lebbou, P. Lecoq, E. Auffray, Journal of Instrumentation 8 (2013) 10017, <http://dx.doi.org/10.1088/1748-0221/8/10/P10017>.
- [17] K. Pauwels, C. Dujardin, S. Gundacker, L. Lebbou, P. Lecoq, M. Lucchini, F. Moretti, A.G. Petrosian, X. Xu, A. Auffray, Journal of Instrumentation 9 (2013) 09019, <http://dx.doi.org/10.1088/1748-0221/8/109/P09019>.